International Journal of
Plasma Environmental Science and Technology

Regular Paper

DOI: 10.34343/ijpest.2023.17.e02002

Novel method for plasma etching of printed circuit boards as alternative for fluorocarbon gases

Wolfram Kintzel[1, *], Marvin Schmid[1], Achim Rentschler[2], Jörg Eisenlohr[2], Volker Bucher[1]

[1] Hochschule Furtwangen, Institute for Microsystems Technology (iMST),
Jakob-Kienzle-Str. 17, 78054 Villingen-Schwenningen, Germany
[2] Plasma technology GmbH, Marie-Curie-Straße 8, 71083 Herrenberg-Gültstein, Germany

* Corresponding author: wolfram.kintzel@hs-furtwangen.de (Wolfram Kintzel)

Received: 08 December 2022
Revised: 26 April 2023
Accepted: 14 June 2023
Published online: 16 June 2023

Abstract

This paper describes a novel method for plasma etching of printed circuit boards (PCBs), replacing climate-damaging perfluorinated Hydrocarbons (HFCs) such as tetrafluoromethane (CF_4). In our alternative process, reactive fluorine would be generated from an inert precursor like commercial PTFE (polytetrafluoroethylene) by means of low-pressure oxygen plasmas. The released fluorine would further be applied to PCB as etchant. Excess fluorine could be chemically absorbed and re-used as recycled precursor later in order to gain a process free of fluorine emissions. Diverse tests were carried out in a lab-scale RF plasma device. We considered different precursor types and examined the plasma composition by means of real-time mass spectrometry. We also determined etch rates on epoxy resin samples by means of mass loss measurements. Process gas composition, precursor type and plasma power were varied, including comparative tests applying state-of-the-art CF_4-O_2-plasma. The efficiency of the etching process was proven. The environmental impact of the novel method was discussed and evaluated regarding PTFE production and greenhouse gas emissions.

Keywords: Printed circuit board, plasma etching, fluorocarbon, PCB, HFC, PTFE.

1. Introduction

Worldwide emissions of perfluorinated hydrocarbons provide a considerable contribution to the global climate change due to their extremely high global warming potential (GWP) and their outstanding persistence. 30 years ago, they were promoted as alternative for ozone-depleting chlorofluorocarbons (CFCs) and widely used in air conditioning and cooling systems, foams, aerosol tins, insulating materials and fire extinguishers. However, these compounds had been rightly regulated since the 2016 Kigali climate conference at the latest. There, a stepwise reduction by 85% until 2036 for industrial countries and by 80% - respectively 85% - for developing and threshold countries until 2047 had been resolved [1]. These targets are primarily connected with the fast growing demand for air conditioning systems, where several substitutes as ammonia, carbon dioxide or propane are already available. Yet those provisions are equally valid for industrial production systems. HFCs are widely used and released in the semiconductor industry and in printed circuit board production for dry and plasma etching processes. Gases used for etching such as tetrafluoromethane (CF_4), hexafluoroethane (C_2F_6), perfluoropropane (C_3F_8) and perfluorobutadien (C_4F_6) have a GWP as high as 7,390 (CF_4) to 12,200 (C_2F_6) [2]. From a technological point of view, plasma etching plays a crucial role in the PCB and semiconductor production. The reasons are increasing demands for the quality of connection areas and a growing complexity of circuits. In PCB applications, back etching of circuit layers in multilayer PCBs, surface activation and structuring or cleaning of drill holes for interconnections represent a few examples. Another essential drawback is that only a small amount of the HFCs is effectively chemically converted in the processes, while around 85% are released worthless in the exhaust [3].

Alternative, HFC-free process gases, which provide appropriate etch rates, process stability and results are not available. The same applies to cleaning systems for an effective and energy efficient removal of fluorine species from the exhaust. Thus, the essential reduction of HFCs could lead to a serious problem for the PCB and semiconductor sector soon. This applies not only for Europe, but also worldwide. Due to confidentiality reasons, no figures for the consumption of HFCs in the PCB and semiconductor industry are available, but can be calculated from other data:

HFC emissions from the German PCB industry was estimated to be 2.0 tons per year in 2008 [4]. The market share of Germany in that year was 1.6% of the global PCB industry [5]. The overall turnaround of the global PCB sector was 60.42 billion US-$ for 2017 [6]. Assuming an annual sector growth rate of 5% between 2008 and 2020 and a constant emission rate, the global HFC emissions would be 224 tons for 2020, corresponding to 1.66 million tons CO_2eq for CF_4. This is an equal greenhouse gas emission as from more than 850,000 mid-size cars in one year (anticipating 130 g CO_2 km^{-1} and 15.000 km p.a.), which illustrates the savings potential in this branch.

The authors propose a novel method for the on-site generation of fluorine gases for plasma etching, exemplarily shown for PCB applications. Our goal is to enable a climate-neutral plasma process that requires no HFC feed, free of primary greenhouse gas emissions. Therefore, we suggest a closed loop plasma process, consisting of the three following steps:

1. Generation of reactive fluorine from a precursor
2. Etching process with fluorine from step 1 and added oxygen
3. Chemical reaction of abundant fluorine species and return as recycled precursor

In this paper, we describe our investigations for the generation of fluorine and fluorine species from a precursor like PTFE (step 1) and its etching behavior to PCBs (step 2) in comparison to the established CF_4-O_2 process. The recycling of fluorine species (step 3) could be realized by plasma treatment of excess process gas with ammonia (NH_3) to form solid ammonia fluoride and/or by reaction with a suitable calcium compound in a separate absorber tank. The resulted solids could be re-used as secondary precursor later.

2. Experimental

2.1 Plasma device configuration

Our plasma system used for all experiments described in this paper consists of a ISO-K 6-way cross vacuum chamber (approx. volume 10 dm^3), a 76 mm diameter × 150 mm length hollow cathode and a 50 kHz HF power generator (type PE-1000 Advanced Energy). Furthermore, we used a Leybold D65BCS backing pump and a turbo pump Leybold Turbovac 50. The system was completed with a gas system for O_2 and Ar or CF_4 (Ar and CF_4 using the same MFC) and a mass spectrometer Pfeiffer Vacuum QMG 250 PrismaPro (1 – 100 u) for residual gas analysis. The mass spectrometer is equipped with an integrated turbo pump, a pressure gauge and includes a software PV MassSpec (V19.12.02-a). Two common PCs were used as control system and for data collection and visualization. A schematic overview of the experimental set-up is shown in Fig. 1. A picture of the set-up is displayed in Fig. 2. Fig. 3 (left) shows the open chamber with the hollow cathode and a PTFE-rod in the center. Fig. 3 (right) displays a view from outside the chamber while an oxygen plasma is burning.

2.2 Fluorine precursor

The impact on oxygen plasma on Polytetrafluoroethylene (PTFE) has been studied since the beginning of our century, showing the principal possibility of PTFE plasma treatment. The focus of these works was the surface modifications of PTFE, e.g. in order to change wettability properties or making the material printable [7]. A former work at our institute also investigated the decomposition of PTFE with oxygen plasma, using it as a source for reactive fluorine species. Thus, we chose PTFE as precursor for an alternative fluorine etch process for the following reasons:

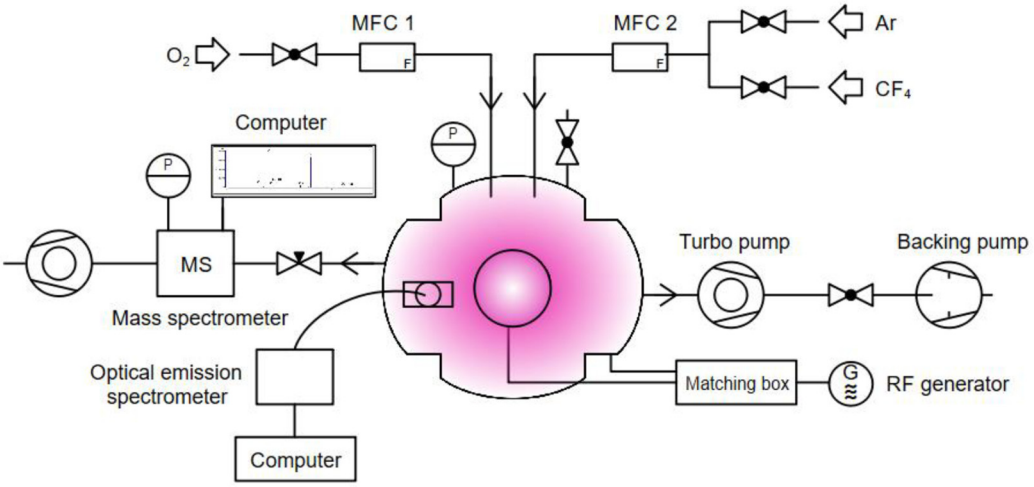

Fig. 1. Scheme of experimental plasma device configuration.

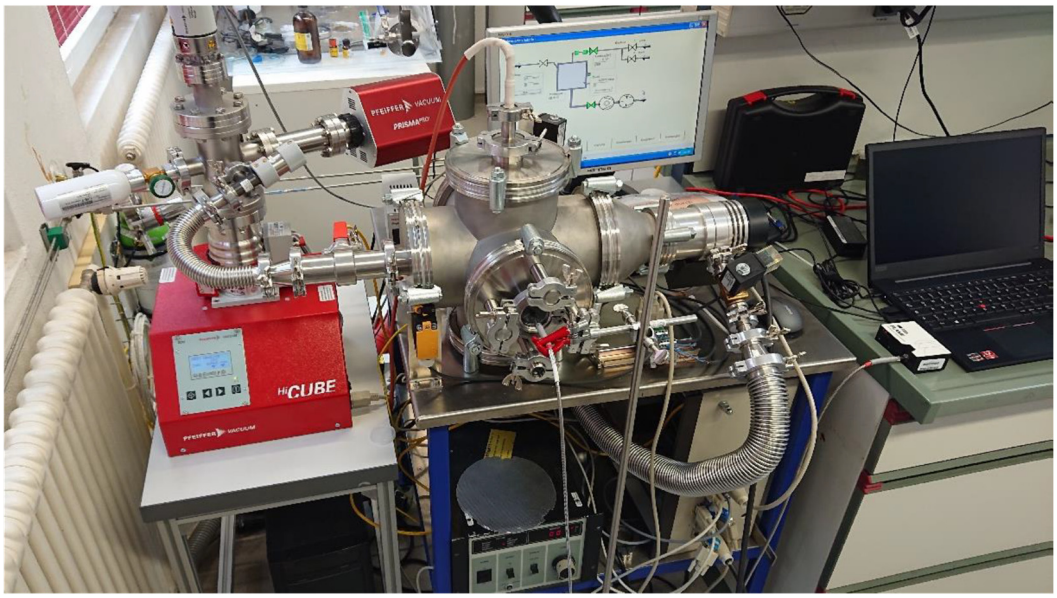

Fig. 2. Principle of ionic wind generation in the MF-DBD plasma actuator.

Fig. 3. On the left: opened plasma chamber with hollow cathode and PTFE-rod in its center. On the right: closed chamber, view from the outside through inspection window, oxygen plasma.

- Commercially available in different shapes, high purity and almost any quantity from many suppliers
- Reasonable price
- Easy and safe handling, nontoxic and inert, stable compound, unlimited storage
- Well-known and industrially proven material since several decades
- Consists only of fluorine and carbon, hydrogen-free
- Principal ability of decomposition by means of plasma

In order to study the impact of the surface, we considered different types and shapes of the polymer, which are listed in Fig. 4. We surveyed the commercial availability including prices and calculated the specific surface. Selected PTFE tubes and bars we purchased from PTFE Nünchritz GmbH & Co. KG, D-01612 Glaubitz and High-tech-flon / Thomas Fahrner & Goran Vlajic GbR, D-78467 Konstanz. Porous PTFE rods and honeycomb bodies were received from ElringKlinger Kunststofftechnik GmbH, D-74302 Bietigheim-Bissingen. Spherules were rejected due to complicated handling. Pall rings are generally injection-molded parts and therefore only commercially available in PFA (perfluoralkoxy alkane), not in PTFE. Thus, they were not used in this work either. Precursor dimensions are resumed in table 1. We assumed a relationship between precursor mass loss and quantity of released active fluorine species. Therefore, the first tests were carried out in determination of mass loss of different precursor types after oxygen plasma treatment in order to compare them.

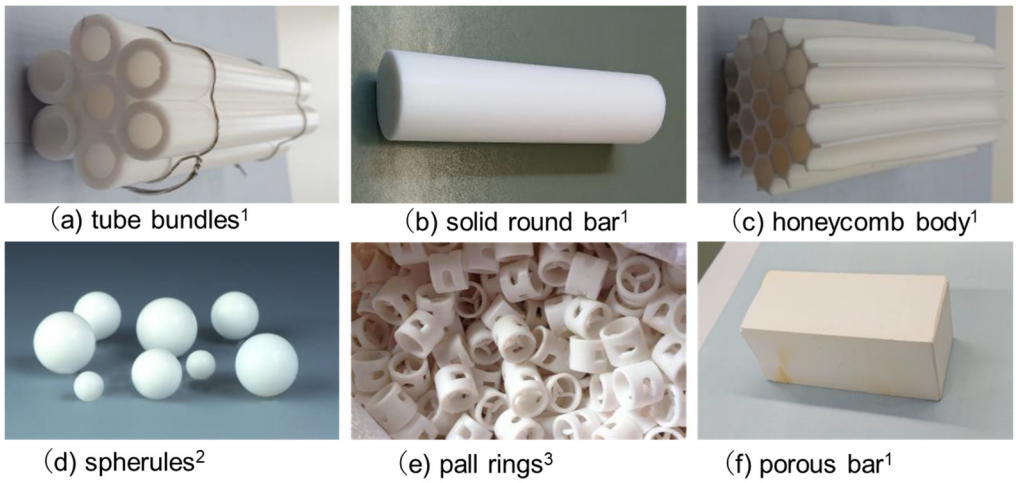

Fig. 4. Different types of PTFE (photo credits: 1 = own, 2 = by kind permission of Bohlender GmbH, D-97947 Grünsfeld, 3 = by kind permission of Ningbo TCI Environmental Protection Co., Ltd, Ningbo city, China 315000).

Table 1. PTFE-precursor dimensions ([4]OD = overall diameter).

PTFE precursor	Outer diameter (mm)	Inner diameter (mm)	Length (mm)	Number of tubes	Surface (cm^2)	Remark
Solid round bar	30	0	120	1	113	
Tube bundle	14	10	140	7	800	
Honeycomb body	15	12	120	19	1300	OD[4] = 70 mm
Porous bar	3535	0	90	1	152	Squared

2.3 Gases

Process gases (oxygen and CF4) were in 5.0 quality, delivered from Linde AG, D-70499 Stuttgart.

2.4 Samples

Two types of samples were used to examine etch rates: Polyamide 6.6 and solidified epoxy resin without fillers. We received the polyamide samples from Rocholl GmbH, D-74927 Eschelbronn, and the epoxy resin samples

from ebalta Kunststoff GmbH, D-91541 Rothenburg o.d.T. The sample dimensions were approx. $25 \times 100 \times 4$ mm^3 for both types. The polyamide samples were received ready-to-use cut from the vendor. The epoxy samples were cut in our lab with a band saw and individually measured in order to enhance accuracy. The etch rate was calculated by weight loss. The surface of each sample was calculated by measuring its dimensions. We employed an analytical balance (KERN ADB 200-4, reproducibility 0.2 mg), weighing before and after plasma treatment. The samples were thoroughly cleaned by hand with isopropanol and dried with nitrogen before each experiment.

2.5 Test configuration

The precursors were placed in the center of the hollow cathode, fixed with a stainless steel (V4A, 1.4401) wire in the first experiments. Later, the stainless steel mount was replaced by a half shell made of quartz, gaining an enhanced stability and centering. The samples were placed at the center on the bottom of the plasma chamber below the hollow cathode, with no direct contact to the plasma. Mass spectrometer measurements of the residual gas in the plasma chamber were started by opening the related valve and adjusting the pressure in the spectrometer with a needle valve. When the measured signal stabilized, plasma was ignited, and the pressure was kept constant manually during measurement. Dwell time was normally 64 ms for a single atom mass. The measurement was carried out in continuous mode, scanning mass-to-charge ratio (m/z) from 1 – 100 u, with activated multiplier. For quantification, the individual signals from mass species were normalized by division through the identified base peak.

2.6 Process parameters

In our experiments, we applied the following parameter setting:

- Chamber pressure: base pressure < 0.01 Pa, process pressure < 5 Pa, typically 1 – 2 Pa
- Gas flows: O_2: 50 sccm
  O_2 / CF_4: [45 sccm O_2 + 5 sccm CF_4 (90:10)] or [40 sccm O_2 + 10 sccm CF_4]
- Mass spectrometer: base pressure < 3. 10-7 mbar, operating pressure = 8. 10-6 mbar,
  dwell time = 64 ms, delay time = 6864 ms
- Plasma power: 100 W – 500 W
- Power density: 0.010 – 0.050 W cm^{-3} (related to chamber volume)
  0.147 – 0.735 W cm^{-3} (related to hollow cathode volume)
- Process time: 10 min in most experiments

We chose an O_2/CF_4 ratio of 90/10 as reference since this is the most common mixture used for PCB etching [8].

3. Results

3.1 Precursor

Oxygen plasma treatment of precursors at 200 W plasma power and 18 minutes process time each resulted in a mass loss shown in Fig. 5. Absolute and relative (surface-related) mass loss was calculated. The figures show that absolute mass loss for all types of PTFE was almost similar (33 to 39 mg min^{-1}), except for honeycomb bodies where only 22 mg min^{-1} was achieved. The surface-related mass loss showed high differences. The solid round bar gave the highest rate of 29.5 mg dm^{-2} min^{-1}, followed by porous PTFE with 22 mg dm^{-2} min^{-1}. Tube bundles and honeycomb bodies performed much worse with 4.4 and 1.7 mg dm^{-2} min^{-1}, respectively

3.2 Etch rates on epoxy resin samples

After applying a 300 W plasma for 10 or 20 minutes on epoxy resin sheets, we calculated etch rates R from weight loss, which was between 4 and 22 mg per sample, and related standard deviation SD. Results are shown in Table 2. The ratio was calculated by division of the etch rate with precursor to the etch rate without precursor

(pure O_2 plasma). Etch rates on polyamide samples gave similar results but were not considered further in this paper since they are probably not relevant for later applications of PCB etching.

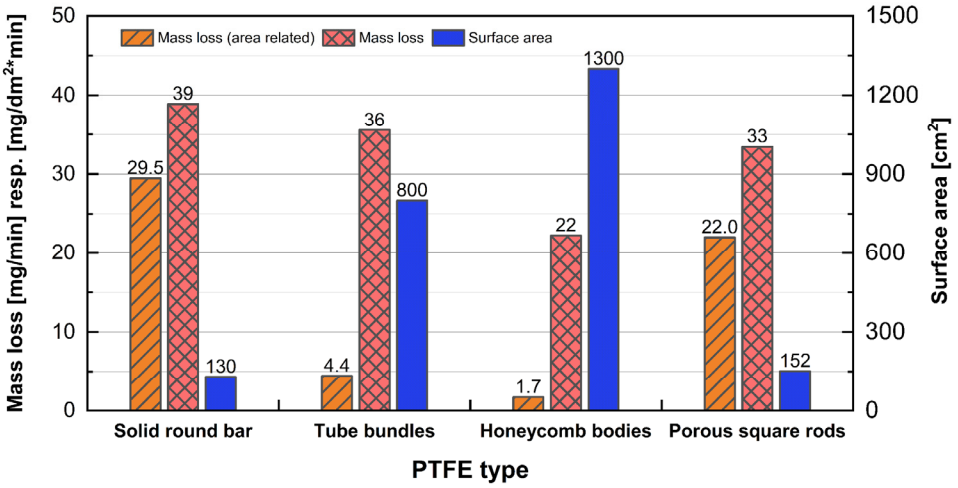

Fig. 5. Absolute and relative mass loss of different precursors after oxygen plasma treatment and related surface.

Table 2. Etch rates on epoxy resin samples.

Precursor	R (µm min^{-1})	SD (%)	Ratio
None (only O_2)	0.19 ± 0.06	34	1.00
CF_4/O_2 (5 + 45)	0.28 ± 0.01	2.7	1.55
PTFE solid bar	0.27 ± 0.02	8.5	1.52
Porous PTFE	0.30 ± 0.08	28	1.66

3.3 Mass spectrometry analysis of plasma species

3.3.1 Identification

Our device basically allowed only measurements of stable plasma chemistry products, which were ionized directly or dissociatively inside the spectrometer. Thus, an interpretation of the fragmentation pattern of those compounds is required and will be discussed in the next chapter of this paper. We identified the relevant species in plasmas fed with pure oxygen, O_2-CF_4-mixture (90/10 by volume) and oxygen using PTFE as precursor. The spectra with raw data as collected are shown in Figs. 6, 7, 8 and 9. We also analyzed the composition of the residual atmosphere without any feed gas and no plasma (see Fig. 6). O_2 molecules have the highest density in all processes and the ions due to their direct (O_2^+ at mass 32 u) and dissociative (O^+ at mass 16 u) ionization are, as expected, the most abundant ions in the spectra of all three plasmas. The O_2^+ peak as one of the highest peaks was used as related signal but has to be normalized before being appropriate as reference, which is discussed in detail in chapter 3.3.3. Water H_2O (OH^+ at 17 u and H_2O^+ at 18 u), carbon monoxide CO (C^+ at 12 u, CO^+ at 28 u), carbon dioxide CO_2 (C^+ at 12 u, CO^+ at 28 u, CO_2^+ at 44 u) were most abundant. The mass spectra from the CF_4- O_2- and the PTFE-O_2- plasma differ slightly from each other. There, additional peaks from carbon ion (C^+, 12 u) fluorine ion (F^+, 19 u), hydrogen fluoride ion (HF^+, 20 u), carbon monofluoride ion (CF^+, 31 u), carbonyl monofluoride ion (COF^+, 47 u), carbon difluoride ion (CF_2^+, 50 u), carbonyl fluoride ion (COF_2^+, 66 u) and carbon trifluoride ion (CF_3^+, 69 u) occurred. In the spectra from O_2-CF_4-plasma, a small peak from F_2^+ ion (38 u) could also be detected. These ions and also other $C_xF_y^+$ ions with higher masses originate from the direct or dissociative ionization of stable C_mF_n molecules formed in the plasma chemistry. CF_4^+ ion was not detected at all. Further, higher mass carbon fluorides ions of type $C_xF_y^+$ such as $C_2F_2^+$ (62 u), $C_3F_2^+$ (74 u), $C_2F_3^+$ (81 u), $C_3F_3^+$ (93 u) or $C_2F_4^+$ (100 u) were not found either. This could also be applied to corresponding CO_mF_n products.

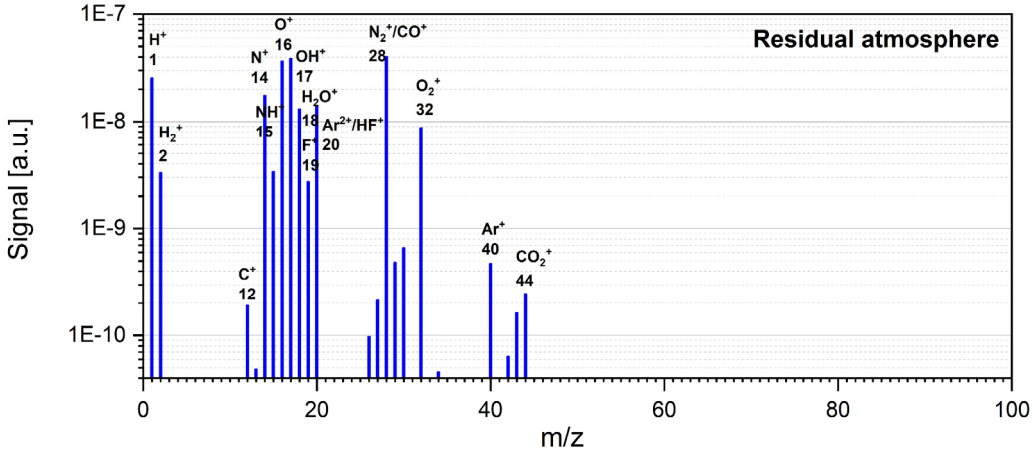

Fig. 6. Mass spectra from residual atmosphere (no plasma, no gas flow).

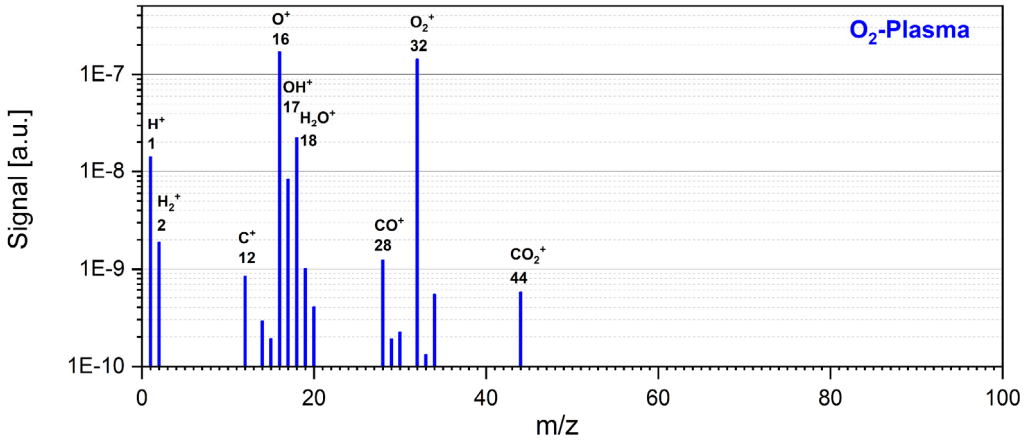

Fig. 7. Mass spectra from oxygen plasma.

We consider the fluorine-containing ions F^+, F_2^+, CF^+, CF_2^++, CF_3^+, COF^+ and COF_2^+ as being the most important indicators of the presence of the products of the PTFE etching process and therefore focused on them in the following discussion. In the residual atmosphere, nitrogen (N_2^+ at 28 u and N^+ at 14 u), oxygen (O_2^+ at 32 u and O^+ at 16 u) and water H_2O (OH^++ at 17 u and H_2O^+ at 18 u) were most common. Smaller amounts of argon (Ar^{2+} at 20 u and Ar^+ at 40 u), hydrogen (H^+ at 1 u and H_2^+ at 2 u), fluorine (F^+ at 19 u), hydrogen fluoride (HF^+ at 20 u) and carbon dioxide (C^+ at 12 u, CO^+ at 28 u, CO_2^+ at 44 u) were detected.

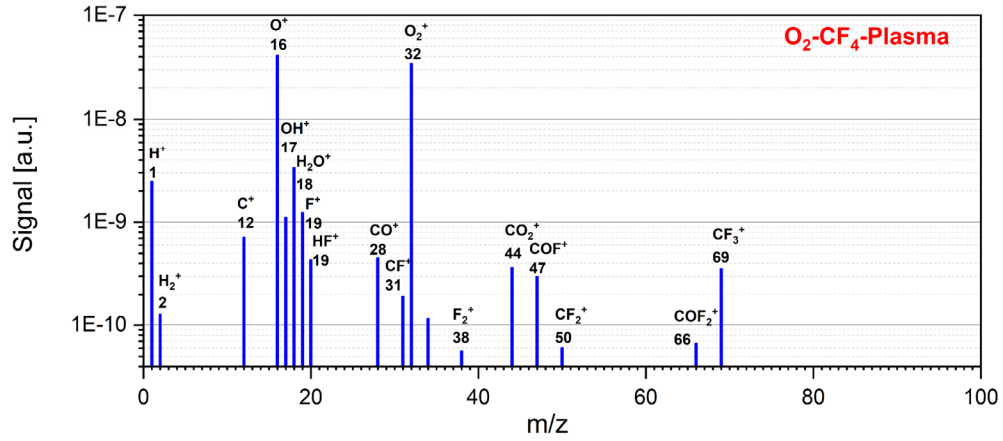

Fig. 8. Mass spectra from residual atmosphere (no plasma, no gas flow).

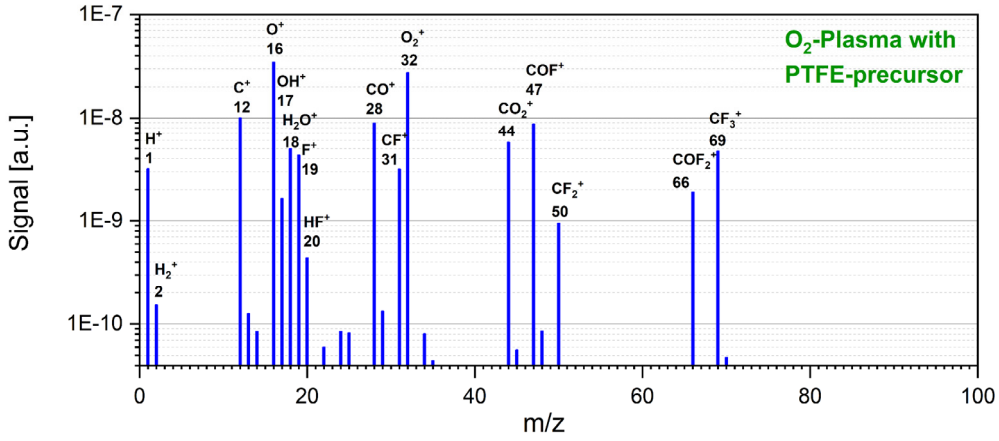

Fig. 9. Mass spectra from oxygen-PTFE plasma

3.3.2 Quantification and time curve

For making the different signals comparable and to compensate pressure variations, they were divided by the O2+ signal. Further normalization is described in chapter 3.3.3. Average values were calculated over process time with plasma, after stabilization. As the various species have different sensitivities to the measurement system, a true quantification would require calibration standards for each species, which would be a tremendous effort. For simplification, we assume an equal selectivity for each species. We believe that the resulted error is tolerable and not significant for later applications

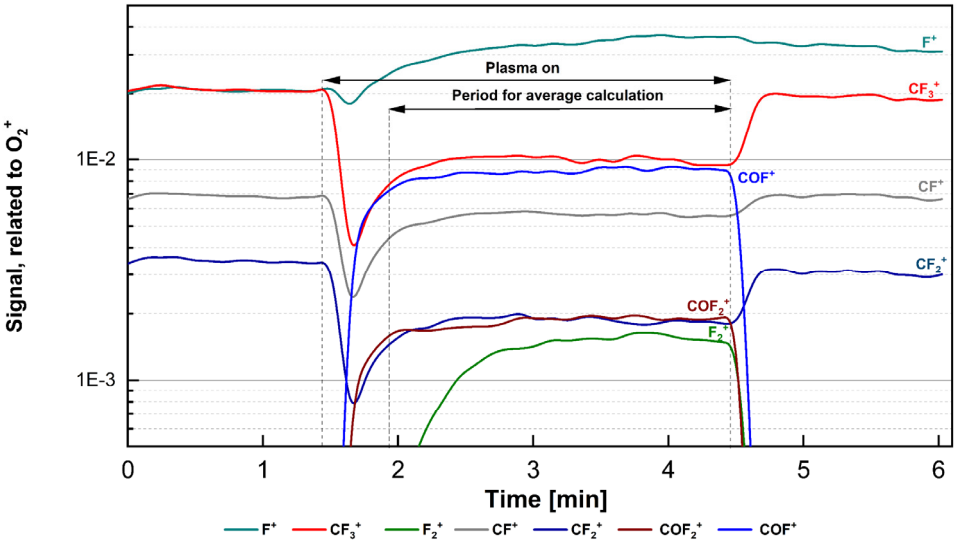

Fig. 10. Time curve of fluorine-containing ions in an oxygen(O_2)-tetrafluoromethane(CF_4)-plasma at 300 W (smoothed).

The quantitative composition of O_2-CF_4- and PTFE-O_2-Plasma was different (see Fig. 10, compared to Fig. 11). The composition of plasma from diverse PTFE types (solid round bar vs. porous PTFE) was quite similar (not shown). As shown in Fig. 10 for CF_4-O_2-Plasma, F^+, CF^+, CF_2^+ and CF_3^+ ions were present with and without plasma. In contrast, COF^+, COF_2^+ and F_2^+ were only present with plasma. CF^+ and CF_2^+ were somewhat decreasing with plasma, whereas CF_3^+ heavily decreased. F^+ was increasing with plasma. After a short period of initialization (20 – 30 s), the signals reached a plateau. In case of F^+ and F_2^+, the initialization seems to be longer (80 s). F_2^+ was detected on a relatively low level

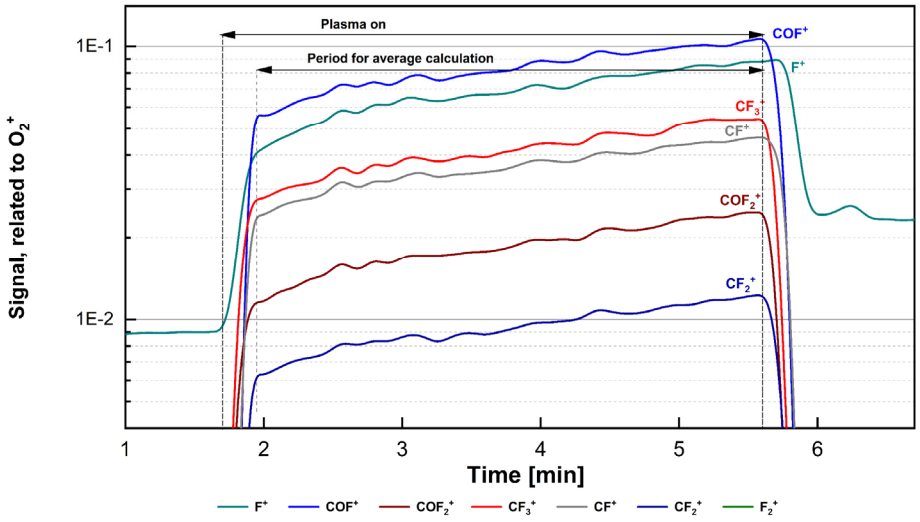

Fig. 11. Time curve of O_2^+ (32 u) signal for O_2-PTFE (solid bar) and O_2-CF_4-plasmas at different plasma powers (smoothed).

3.3 Signal normalization

In theory, more oxygen was consumed in PTFE plasmas than in CF_4 plasmas due to different chemistry and higher stability of CF_4 compared to PTFE. We verified if the different level of O_2 consumption has to be considered in the interpretation of the data by comparing the O_2^+ signal development during plasma process of O_2-CF_4 and O_2-PTFE plasmas at various plasma power. The results are shown in Fig. 12.

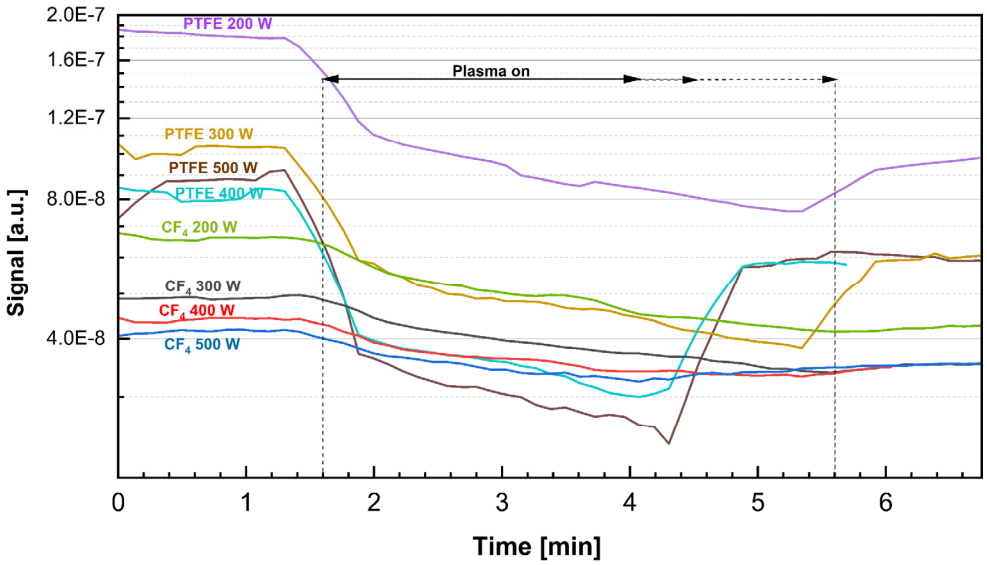

Fig. 12. Time curve of O_2^+ (32 u) signal for O_2-PTFE (solid bar) and O_2-CF_4-plasmas at different plasma powers (smoothed).

The measurements show a significant drop of the O_2^+ signal for the PTFE plasmas after plasma was turned on, whereas in case of the CF_4 plasmas only a slight decrease was observed. The signal drop seemed to be higher with increased plasma power. The initial O_2^+ signal in case of PTFE was somewhat higher than for CF_4. This reveals that the O_2^+ signal drop was caused by a change of O_2 density in the reactor and this density change has to be considered for the signal normalization. First, the signal intensity could be divided by the O_2 gas flow, leading to a corrected, O_2 gas flow related signal. This is also important for considering different O_2 gas flows for the experiments employing CF_4 and PTFE. Second, the change of O_2 density during plasma on with PTFE shall be considered by introducing a corrected O_2 gas flow, calculated for different plasma power.

The corrected O_2 gas flow V_{corr} was calculated by the following equation, where V_0 is the nominal O_2 gas flow, i_0 is the average raw signal before the plasma was turned on and i_1 is the average raw signal during plasma turned on:

$$\dot{V}_{corr} = \dot{V}_0 \times (1 - \frac{i_0 - i_1}{i_0}) \quad (1)$$

Results for different plasma powers are shown in Table 3. Additionally, the initial O_2^+ signals of PTFE for different plasma powers differed somewhat from each other, especially at the 200 W setting. We suspect a temperature effect as the cause, namely that the plasma chamber was not completely and uniformly warmed up at the beginning of the test series. However, we consider the differences of the initial absolute values to be less important; what is decisive is the relative signal drop after the plasma was switched on.

Table 3. Average O_2^+ signal change and corrected O_2 gas flows for different PTFE plasmas.

Power (W)	200	300	400	500
O_2 gas flow, nominal = $\dot{V}_0$ (sccm)	50	50	50	50
O_2^+ raw signal, average, before plasma on = i_0 (a.u.)	1.81×10^{-7}	1.03×10^{-7}	8.22×10^{-8}	8.83×10^{-8}
O_2^+ raw signal, average, during plasma on = i_1 (a.u.)	8.82×10^{-8}	4.57×10^{-8}	3.46×10^{-8}	3.07×10^{-8}
O_2^+ raw signal change percentage	−51%	−56%	−58%	−65%
O_2 gas flow, corrected = $\dot{V}_{corr}$ (sccm)	24.2	22.1	21.0	17.4

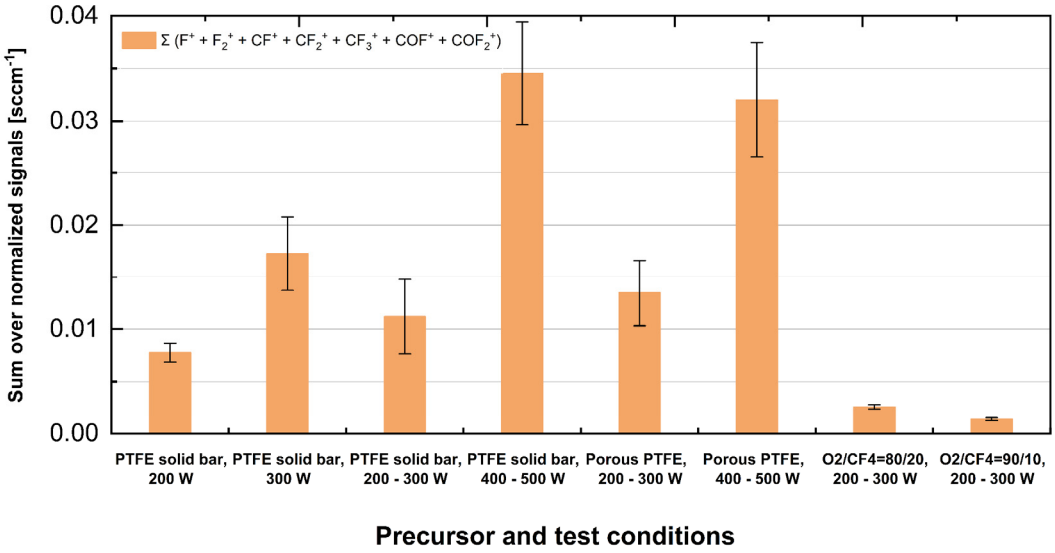

Fig. 13. Sum over signals of fluorine-containing ions (F^+, F_2^+, CF^+, CF_2^+, CF_3^+ COF^+ and COF_2^+) for different precursor with various parameters (normalized to O_2^+ signals and corrected O_2 gas flow).

3.3.3 Sum over normalized signals of fluorine-containing ions

A comparison of the sum over normalized signals of fluorine-containing ions for different precursor and various power input showed noticeable differences (see Fig. 13). With higher power, the sum increased in case of the PTFE precursor. At high power, no difference between solid and porous PTFE was measured, whereas at lower power, the porous PTFE resulted in a significant higher quantity of fluorine-containing ions. In contrast, the figures for CF_4 plasmas were much lower.

Beyond, the direct correlation of the sum over normalized signals of fluorine-containing ions and plasma power was examined. Results are shown in Fig. 14. For both PTFE types (solid and porous), a light polynomic growth, following a quadratic function, was proven. For CF_4, the results were different. An almost linear,

delicate increase was observed, reaching its maximum at 300 W. Further increase of power up to 500 W resulted in no further amount of species.

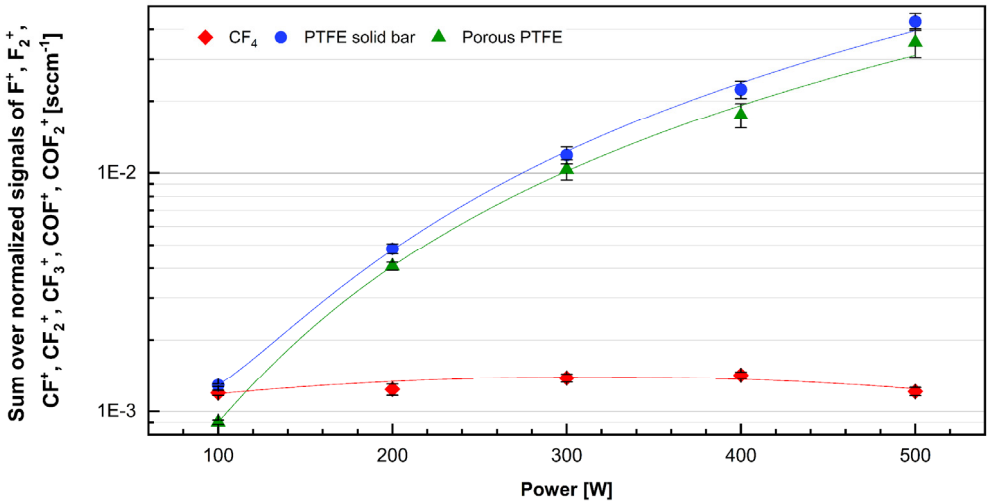

Fig. 14. Sum over normalized signals of fluorine-containing ion species vs. plasma power (normalized to O_2^+ signals and corrected O_2 gas flow) for PTFE- and CF_4-plasmas.

3.3.4 Distribution of fluorine species

Almost 40 tests were carried out with variation in precursor type and plasma power to examine the share of the individual fluorine ion species. The summarized results are shown in Table 4. The most abundant ion species in PTFE-plasmas was COF^+, whereas in CF_4-plasmas it was F^+. In CF_4 plasmas, CF_3^+ and COF^+ were the second most common species. In PTFE plasmas, the second most frequent species were CF_3^+ and F^+. CF^+ was on the forth rang in all plasmas.

Table 3. Relative share of fluorine-containing ion species for different prec.

Precursor	Relative share (%)						
	F^+	F_2^+	CF^+	CF_2^+	CF_3^+	COF^+	COF_2^+
PTFE	17.4 ± 15.6	0.09 ± 0.11	14.0 ± 13.3	4.3 ± 3.8	18.0 ± 15.8	37.6 ± 33.1	8.7 ± 7.3
CF_4/O_2 = 90/10	33.2 ± 6.3	1.4 ± 1.1	10.3 ± 1.2	4.0 ± 0.9	21.6 ± 6.5	24.5 ± 3.1	5.1 ± 0.7

CF_4 plasmas had a significantly higher fluorine (F^+) content than PTFE plasmas. In most of the investigated plasmas, the further order of abundance was COF_2^+ and CF_2^+. The rarest ion species was always F_2^+. Its proportion was very clearly higher in CF_4 plasmas than in PTFE plasmas. The standard deviation (SD) of the ion species content in CF_4 plasmas was distinctly lower than that in PTFE plasmas. In PTFE plasmas, the SD of COF^+ was relatively high. With low power, the SDs of all species were considerably lower than that with medium or high power. We also investigated the plasma composition in correlation to plasma power. The results are subsumed in Figs. 15, 16 and 17. With the solid bar PTFE, there was a light increase of CF_2^+, COF^+ and COF_2^+, and a more distinct increase of CF_3^+ with increasing power. F+ was linear decreasing with increasing power. CF^+ was nearly constant or slightly decreasing. F_2^+ was decreasing with increasing power up to 300 W and then staying almost constant. Examining the O_2-CF_4-Plasma, CF^+, CF_2^+ and CF_3^+ were decreasing with increasing power up to 300 W, and then remaining almost steady. F^+, COF^+, COF_2^+ and F_2^+ were rising with increasing power.

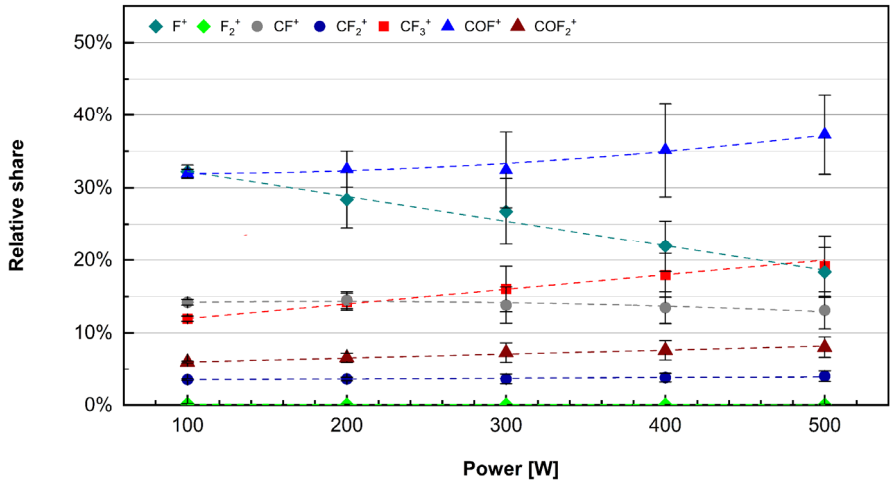

Fig. 15. Relative share of fluorine-containing ion species in an O_2- PTFE (solid bar) plasma as a function of plasma power.

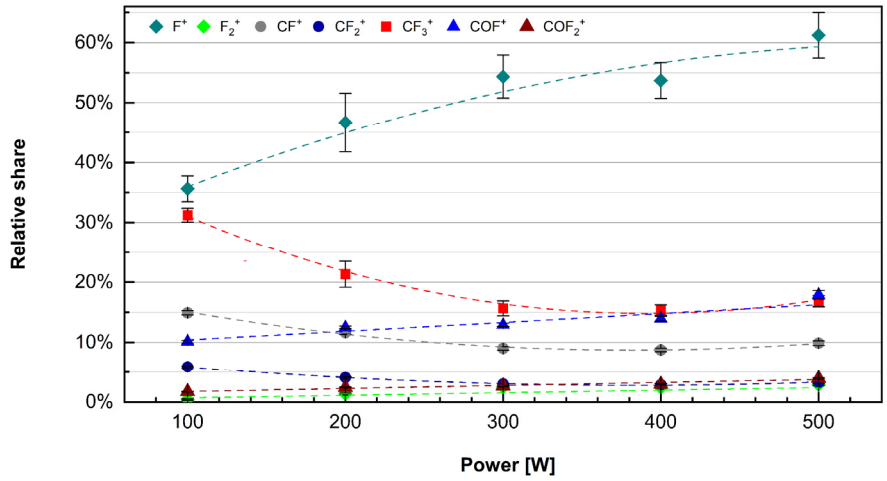

Fig. 16. Relative share of fluorine-containing ion species in an O_2-CF_4 (90:10) plasma as a function of plasma power.

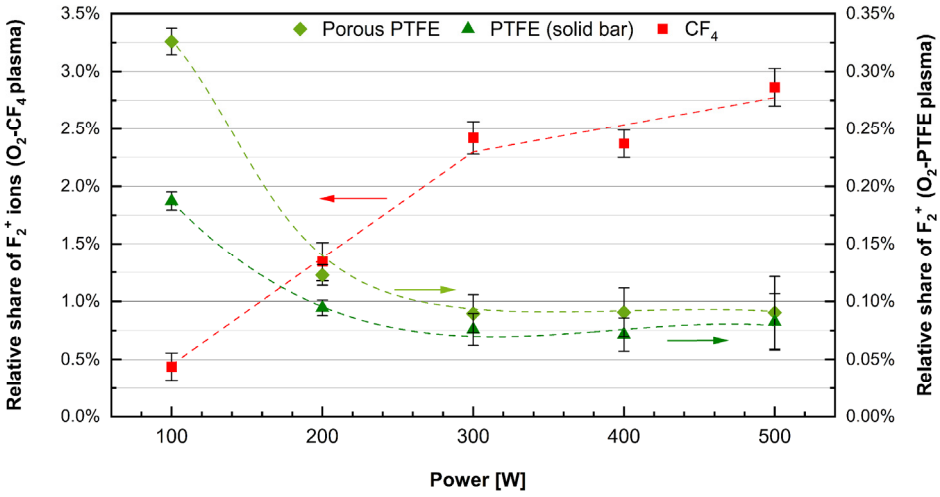

Fig. 17. Relative share of F_2^+ ions in different plasmas as a function of plasma power (left ordinate: CF_4-plasma, right ordinate: PTFE plasmas).

3.3.5 HF^+ content

The relative share of HF^+ ions in the residual gas was calculated as ratio of measured HF^+ ions (20 u) to overall content of all fluorine-containing ion species (F^+, F_2^+, CF^+, CF_2^+, CF_3^+ COF and COF_2^+) including HF^+. We noticed that PTFE plasmas released much less HF^+ than the compared CF_4 plasma in most experiments. The HF^+ amount decreased significantly with increasing power in PTFE plasmas, see Fig. 18. In CF_4 plasmas, the HF^+ content increased rapidly in the lower power range and then stayed on an almost constant level. At low power (100 W), the HF^+ content is very similar for all investigated plasma types.

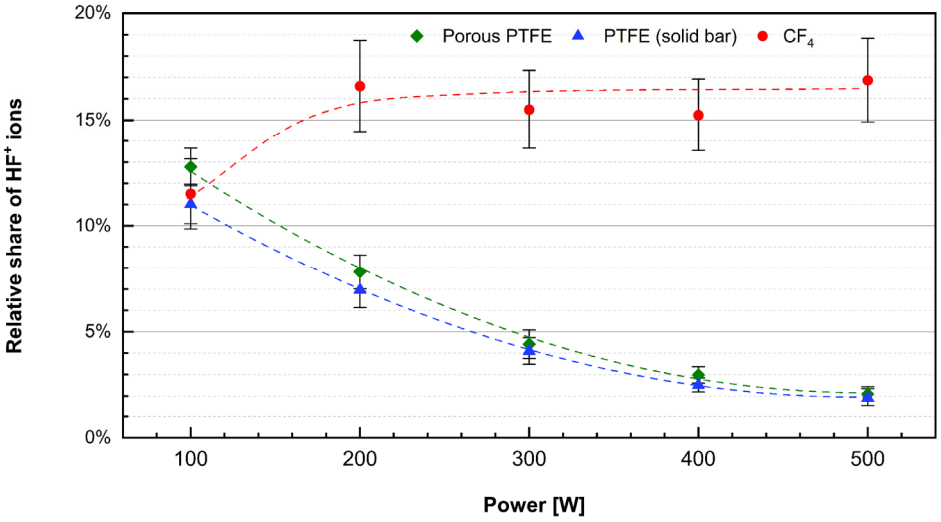

Fig. 18. Relative share of HF^+ ions for different precursor as a function of plasma power

4 Discussion

4.1 Precursor

The surface area of different types of PTFE had almost no impact on the mass loss by plasma. This applies also for the porous PTFE type. Hence, the reaction scheme seemed to be physically transport-controlled in the plasma phase and not reaction-controlled on the solid-plasma interface. Consequently, the need of applying any special shape or modification of PTFE is omitted.

4.2 Etch rates

The etch rate of CF_4 plasma at 300 W power on epoxy resin was 1.55-fold of those with pure oxygen. In comparison, the etch rate ratio of solid PTFE was 1.52 and for porous PTFE it was 1.66. Thus, we conclude that our alternative PTFE process is rather as efficient as the established CF_4 process. Due to a clearly higher standard deviation, the larger value for porous PTFE has limited significance. Possibly, the process with porous PTFE is less stable than with the solid one.

4.3 Mass spectrometry analysis of plasma species

4.3.1 Identification

The mass spectra of CF_4- and PTFE-plasmas are quite similar to each other, regarding their qualitative composition. No species were identified only in one type of plasma. CF_4 was not detected at all, as it is known to be unstable in its ionic state and turned into CF_3^+ and F^+ inside the spectrometer [10, 11]. Higher mass multiple carbon fluorides ions $C_xF_y^+$ were reported in two other studies about CF_4 plasma [11, 12] but not found in some others [10, 13] and in this work. Even with the limited range of our device (1 – 100 u), we did

not find any lower mass species as $C_3F_2^+$ (74u), $C_2F_3^+$ (81 u), $C_3F_3^+$ (93 u) and $C_2F_4^+$ (100 u). We suspect feed gas impurities (e.g., C_4F_8), different measurement methods or different plasma sources as possible reasons. We estimate the impact to be negligible. The residual gas atmosphere was inconspicuous, except for its fluorine (F^+) content. We ascribe this to the adsorption of fluorine on the chamber walls and its slow and continuous release.

4.3.2 Reaction schemes of PTFE

We suggest a reaction scheme for PTFE-O_2-plasmas as described as followed. The scheme shall cover the most likely main reactions, forming a foundation for basic understanding and for further research. It does not claim to be complete.
First, oxygen

$$O_2 + e^- \rightarrow 2O + e^- \quad \text{(R1a)}$$

$$O_2 + e^- \rightarrow O + O(^1D) + e^- \quad \text{(R1b)}$$

Secondly, C-C-bonds of the PTFE polymer chain were cracked by oxygen radicals bombardment onto the polymer surface (C-C-bonds are weaker than C-F-bonds), resulting in tetrafluoroethylene (C2F4), according to R2. C2F4 formation is well known from thermal decomposition of PTFE [14] and could also be assumed for plasma treatment as intermediate compound. However, we could not detect any C2F4 in the mass spectra. A reasonable explanation is fragmentation in the spectrometer according to R17 to R19 (beside reaction with oxygen in the plasma).

$$[CF_2]_n + O(^1D) \rightarrow n/2\ C_2F_4\uparrow + O \quad \text{stable} \quad \text{(R2)}$$

Then, the following main reactions probably occurred in the plasma:

$$C_2F_4 + 2O \rightarrow CF_4 + CO_2 \quad \text{stable} \quad \text{(R3)}$$

$$C_2F_4 + 2O \rightarrow 2COF_2 \quad \text{stable} \quad \text{(R4)}$$

$$C_2F_4 + 2O \rightarrow COF + COF_2 + F \quad \text{partially stable} \quad \text{(R5)}$$

$$C_2F_4 + O \rightarrow CF_4 + CO \quad \text{stable} \quad \text{(R6)}$$

$$CF + O \rightarrow COF \quad \text{unstable} \quad \text{(R7)}$$

$$2CF_3 + 2O \rightarrow COF_2 + COF \quad \text{partially stable} \quad \text{(R8)}$$

$$COF_2 + O \rightarrow CO_2 + 2F \quad \text{partially stable} \quad \text{(R9)}$$

$$2FO \rightarrow F_2 \quad \text{stable} \quad \text{(R10)}$$

Of these, R2 to R4, R6 and R10 led to stable reaction products, namely C_2F_4, CF_4, COF_2, CO_2, CO and F_2. R5, R8 and R9 led to partially stable ones: COF_2 and CO_2 are stable, COF and F are unstable. Inside the mass spectrometer, the following ionization and cleavage reactions might occur, known as electron-impact ionization or multiple ionization:

$$CF_4 + e^- \rightarrow CF_3 + F + e^- \quad \text{(R11)}$$

$$CF_4 + e^- \rightarrow CF_2 + 2F + e^- \quad \text{(R12)}$$

$$CF_3 + e^- \rightarrow CF_2 + F + e^- \quad \text{(R13)}$$

$$CF_2 + e^- \rightarrow CF + F + e^- \quad \text{(R14)}$$

$$CF_2 + e^- \rightarrow C + 2F + e^- \quad \text{(R15)}$$

$$CF + e^- \rightarrow C + F + e^- \quad \text{(R16)}$$

$$C_2F_4 + e^- \rightarrow 2CF_2 + e^- \quad \text{(R17)}$$

$$C_2F_4 + e^- \rightarrow C_2F_3 + F + e^- \quad \text{(R18)}$$

$$C_2F_3 + e^- \rightarrow CF_2 + CF + e^- \quad \text{(R19)}$$

$$COF_2 + e^- \rightarrow COF + F + e^- \quad \text{(R20)}$$

$$COF + e^- \rightarrow CO + F + e^- \quad \text{(R21)}$$

$$O_2 + e^- \rightarrow 2O + e^- \quad \text{(R22)}$$

$$F_2 + e^- \rightarrow 2F + e^- \quad \text{(R23)}$$

This is corresponding with the amount of detected species.

4.3.3 Quantification and time curve

The time curve of plasma species looked different for CF_4- and PTFE-plasmas. After a short time of initiation, CF_4 plasmas showed a constant level, whereas in PTFE plasmas, a permanent ascent could be measured. CF_4 plasma can be regarded as homogeneous single-phase reaction, PTFE plasma, in contrast, as non-catalyzed heterogeneous reaction of a multiphase system. This could explain these differences. The rise in case of PTFE plasma could be related with temperature increase of the material. After a test cycle, the plasma chamber was noticeable warm and also the PTFE rod was heated up. Thermocouple measurements confirmed this: After 10 min of plasma with 300 W power, a temperature of 98 °C was measured on the PTFE surface. The measurements of CF_4 plasma also revealed that CF_x (x = 1…3) was consumed by the plasma, while C, COF, COF_2, F and F_2 was formed. CF_x species play an important role in the etch process. They act as precursor for F but may also contribute to the formation of undesired polymer film on substrates, etching parts or chamber walls [15]. Considering the results of the O_2^+ signal measurements, the following can be concluded: Even there was a drop in intensity after the plasma was turned on in case of PTFE plasma, there was no significant difference between CF_4- and PTFE-plasmas while the plasma was on. Thus, the evolution of the O_2^+ signals were quite similar and in the first approach, there seem to be no need for a correction of the signal ratios of the investigated species. In later studies, it may be examined in more detail.

4.3.4 Total amount

The overall amount of fluorine species of PTFE plasmas could increase by elevating power, whereas in CF_4 plasma only little raise was measured, reaching a maximum at medium power. The limiting factor in CF_4 plasmas seemed to be the availability of gaseous CF_4, which is directly correlated with feed gas flow and limited by the required pressure regime. The higher total amount of fluorine species in PTFE plasmas could lead to a higher etching rate. The correlation between power and total amount of species might enable a suitable control of the etching process by adaption of plasma power. We noticed no significant difference between solid and porous PTFE. In contrast to our presumptions, we saw no considerable advantages by using porous PTFE. This means, much cheaper standard-PTFE could be applied.

4.3.5 Distribution of fluorine-containing ion species

CF^+ concentration in our plasma was always higher than CF_2^+, which is in contrast to other publications [9, 16]. One reason could be that these researchers investigated ICP plasmas, applying 13.56 MHz sources, including different chamber and experimental designs. Another reason might be the ionization and cleavage of C_2F_4 inside the spectrometer according to R17. Therefore, different results are not surprising. CF_x^+ species play an important role in etching processes as they act as precursor for atomic fluorine. On the other hand, they contribute to the formation of unfavorable polymer films [15]. The measured CF_x^+ content in our tests was quite similar in both plasma processes. From this aspect, we expect no effects. The slightly higher concentration of C^+ ions in PTFE plasmas has probably no significant impact, especially when considering the high SD values. We measured more COF^+ and COF_2^+ and less F^+ and F_2^+ ion species in PTFE plasmas compared to CF_4 plasmas. We attribute this to a different reaction scheme, as mentioned before in this chapter. In PTFE, C-C bonds must be broken additionally and presumably primarily. This is probably done by O radicals, which reduces the concentration of O^+, so that less F^+ and F_2^+ are formed and more COF^+ and $COF_2^+$are released. Remarkable, F_2^+ concentration was around one order of magnitude higher in CF_4 plasmas. According to other publications [12, 13], F_2 molecules may form in two reactions:

$$F + F \rightarrow F_2 \quad \text{(R24)}$$

$$COF_2 + O(^1D) \rightarrow F_2 + CO_2 \quad \text{(R25)}$$

Thus, if there were more F available this would result in a higher F_2 content. The concentration of F^+ was also higher, but not to the same extend. COF_2^+ was even lower in CF_4 plasmas. It is unclear if there was a difference in the level of excited oxygen ($O(^1D)$) in those plasmas. Hence, further investigations are necessary for a reliable explanation.

4.3.6 HF^+ content

Tezani *et al*. found that HF decreased the concentration of F atoms in plasma [17]. As we found significantly lower HF^+ concentrations in PTFE plasmas compared to CF_4 plasmas, a positive impact on etching rates could be expected. Moreover, HF is an unwanted reaction product due to its corrosive and highly toxic properties. Thus, lower HF values are advantageous with the PTFE process. A significant decrease of HF^+ content with increasing plasma power would make an easy control of HF content feasible.

4.3.7 Functions of plasma power

In porous PTFE plasma, no clear correlation to power input was found, except for F_2^+. In PTFE solid bar plasma, F^+ was somewhat decreasing and COF^+ and COF_2^+ were increasing with power. For both PTFE types, F_2^+ was first strongly decreasing to 300 W and then constant or slightly increasing with power. We suppose that F was consumed to form COF and COF_2 and therefore decreased with increasing power.

In CF_4 plasma, C^+, CF^+ and CF_2^+ were decreasing and F^+, COF^+ and F_2^+ were increasing in the range up to 300 W and then nearly constant with increasing power. F_2^+ showed the strongest correlation. This indicates that a stable equilibrium state was reached, and increased energy input had no significant effect on the composition of the plasma. The formation of COF, F and F_2 were energy-consuming reactions. Thereof we conclude that these species were also more reactive than the others were. Surprisingly, only COF_2^+ showed a special behavior with almost linear increase with power over the complete range. We attribute this to the fact that COF_2 is a stable compound in contrast to all other reactive species (except for F_2).

4.4 Environmental aspects

PTFE synthesis is based on the polymerization of tetrafluoroethene (TFE) monomers (R26), TFE is mainly produced by reaction of chloroform ($CHCl_3$) with hydrogen fluoride (R27a+b). Chloroform results from a reaction of methane and chlorine according to (R28).

$$nC_2F_4 \rightarrow (C_2F_4)_n \quad \text{(R26)}$$

$$CHCl_3 + 2HF \rightarrow CHCLF_2 + 2HCl \quad \text{(R27a)}$$

$$2CHCl_2 \rightarrow C_2F_4 + 2HCl \quad \text{(R27b)}$$

$$CH_4 + 3Cl_2 \rightarrow CHCl_3 + 3HCl \quad \text{(R28)}$$

Chloroform is rated as naturally occurring halocarbon with an annual global turnover of 700,000 tons, whereof less than 10% are from artificial sources [18]. Therefore, it shall not be considered further here. As hydrochlorofluorocarbons (HCFCs) such as chlorodifluoromethane ($CHClF_2$) as intermediate are globally regulated since the 1990s due to their ozone-depleting potential, closed-loop-systems are installed in the industry and HCFC gas emissions are strictly limited and monitored.

The state-of-the-art method for synthesizing PTFE is the free radical polymerization of TFE in an aqueous solution. There are two main processes: suspension polymerization and emulsion polymerization. The latter requires emulsifiers in order to stabilize the generated polymer particles in the liquid phase and is applied, beside others, in the production of fine powder PTFE [19, 20]. For many years, perfluoroalkyl carboxylic acids (PFASs) such as perfluorooctanoic acid (PFOA) and perfluorooctanesulfonate (PFOS) had been applied as emulsifiers. These chemicals had not only been used in the production of fluorinated polymers, but also in a wide range of industrial and consumer products for almost 50 years. However, since the 1990s it became evident that these substances are highly problematic due to their high persistence in the environment and harmfulness to human health, e.g., to liver, development and the immune system. Detectable amounts in human body fluids had been measured in different populations all over the world [21]. Therefore, and consistently, "PFOS and PFOS-related compounds have been largely phased out and were restricted in the EU in 2008" [22].

Substitutes had been developed by different companies. Dyneon, as one of the pioneers, introduced a monohydrofluorocarboxylic acid ammonium salt $[NH_4]^+[CF_3\text{-}O\text{-}(CF_2)_3\text{-}O\text{-}CHF\text{-}CF_2\text{-}COO]^-$, known as ADONA, in their production in 2008 and completely replaced the previously used PFOA ammonium salt (APFO) one year later [19]. Investigations showed that ADONA is faster eliminated from the human body and the toxicological properties are less problematic than those of PFOA are. In one study, just in a few samples values over the limit of detection (0.2 µg L^{-1}) were measured [22]. "Under the U.S: EPA2010/15 Stewardship Program, eight major manufacturers phased out PFOA/PFNA in their fluoropolymer production". However, others still have it in use, especially in China, and it is yet uncertain if PFAS will be replaced industry-wide in the near future [20]. In contrast, granular PTFE is produced differently by suspension polymerization and does not require PFAS as auxiliary agent [20]. Consequently, it is essential to check the origin of the applied PTFE semi-finished product and to choose a reliable, certified manufacturer. Doing so, the proposed alternative process described in this paper can be sustainable.

4.5. Comparison of greenhouse gas emissions

Based on our tests, we try to estimate the greenhouse gas of our alternative process compared to a conventional, CF_4- employing etching process. First, we took our measured PTFE mass loss of 39 mg min^{-1} as requirement, compared with 5 sccm CF_4 consumption, which makes 18.6 mg CF_4 / min. 39 mg related to 18.6 mg results in a factor of 2.1, which means that 2.1 kg PTFE replaces 1 kg CF_4. Based on the calculation in Introduction, the overall HFC consumption would be 263.5 ton yr^{-1}, assuming an efficiency of 15%. This would be equal to 550 ton yr^{-1} of PTFE. The GWP for the production of 1 kg PTFE is 14.44 kg CO_2eq [23], which results in a total of 7,942 t CO_2eq. Furthermore, we assume that 90% of fluorocarbon compounds in our process are effectively used, chemically absorbed or recycled, and just 10% is released into the atmosphere. This would give HFC emissions of 55 ton yr^{-1}, equal to 406,450 ton yr^{-1} CO_2eq. Adding the GWP emissions for PTFE production results in a total of 414,392 ton yr^{-1} CO_2eq. Compared to the emissions from the conventional process (1,655,360 t/a CO_2eq), this is a saving of 1,240,968 ton yr^{-1} CO_2eq corresponding to 75%. If a better retention of 95% is achieved, the reduction in GWP would be 1,444,193 ton yr^{-1} CO_2eq, corresponding to 87%.

Tests with after-treatment applying NH3 plasma showed significant differences between the two processes. With the PTFE process, a considerable amount of a white, solid substance could be collected in a cooling trap; with CF_4, in contrast, only minor traces appeared. This is a clear indication that a high amount of fluorine

components in the PTFE exhaust gas are reactive and therefore easier to remove compared to the very stable CF_4. Detailed results will be reported elsewhere in the near future.

5. Conclusion

The absolute mass loss for different shapes of PTFE was always similar, i.e., almost independent of the surface. Therefore, standard PTFE in rod shape can be used. We investigated the composition of the plasmas by mass spectrometry. The qualitative composition of CF_4- and PTFE plasmas was identical. The quantitative composition was different. We attribute this to different reaction types: The CF_4 plasma is a homogeneous single-phase reaction, while the PTFE plasma is a heterogeneous multiphase reaction. In the case of PTFE plasma, the content of reactive species could be increased by elevating the plasma power, whereas this was not possible in the case of CF_4-plasma. The plasmas also differed in the quantitative composition of the reaction products. In particular, less HF was found for PTFE plasma. The quantitative composition as a function of power was investigated, and minor correlations were found for a few species. With PTFE plasma, almost the same etch rates could be achieved on epoxy samples at the same power as with CF_4 plasma. With porous PTFE, even slightly higher etch rates were obtained, but the results were subject to a higher uncertainty (SD). Since the content of reactive species in the PTFE plasma could be increased by raising the power, even higher etch rates can be expected. In our tests, porous PTFE showed somewhat higher etch rates than solid PTFE, but no advantages were apparent in the composition of reactive species. Moreover, as it is an exotic and expensive PTFE variant, normal, commercially available PTFE in solid rod shape could be applied. As a result, it is possible in principle to generate reactive fluorine components from PTFE by means of plasma and thus to realize an etching process comparable to CF_4. As next steps, further investigations on samples close to the application (PCBs) are planned.

Acknowledgment

The authors would like to thank the Federal Ministry of Education and Research (BMBF) for the financial support of the project “PlasmaKlient” (FKZ: 01LY1915B, funding measure: KMU-innovativ: Ressourceneffizienz und Klimaschutz). We also thank ElringKlinger Kunststofftechnik GmbH for providing free PTFE samples and ebalta Kunststoff GmbH for delivering epoxy resin sheet.

References

[1] United Nations, Amendment to the Montreal Protocol on Substances that Deplete the Ozone Layer, Kigali, October 2016.
[2] Global Warming Potential (GWP) of certain substances and mixtures that contain such substances, based on the Fourth Assessment Report of the Intergovernmental Panel on Climate Change and a hundred years time period, Umweltbundesamt, Dessau-Roßlau, May 2019.
[3] W. Schwarz, A. Leisewitz, Emissions and Reduction Potentials of Hydrofluorocarbons, Perfluorocarbons and Sulphur Hexafluoride in Germany, Umweltbundesamt, Dessau-Roßlau, October 1999.
[4] W. Schwarz, Inventory compilation of F-gases 2008. Data on HFCs, PFCs, and SF6 for the national emissions reporting under the Framework Convention on Climate Change for the reporting year 2008, Umweltbundesamt, Dessau-Roßlau, July 2010.
[5] IPC PCB World Production report 2014.
[6] Global Printed Circuit Board (PCB) Market Outlook, Trend and Opportunity Analysis, Competitive Insights, Actionable Segmentation & Forecast 2024, Energias Market Research Pvt. Ltd., Buffalo New York, December 2019.
[7] Stefano Zanini, Ruggero Barni, Roberto Della Pergola and Claudia Riccardi, Modification of the PTFE wettability by oxygen plasma treatments: influence of the operating parameters and investigation of the ageing behaviour, *J. Phys. D: Appl. Phys*., Vol. 47 (32) 325202 (9pp), 2014.
[8] Becken K., de Graaf D., Elsner C., Hoffmann G., Krüger F., Martens K., Plehn W., Sartorius R.., Avoiding fluorinated greenhouse gases. prospects for phasing out, Umweltbundesamt, Dessau-Roßlau, June 2011.
[9] Fukumoto H., Fujikake I., Takao Y., Eriguchi K. and Ono K., Plasma chemical behaviour of reactants and reaction products during inductively coupled CF_4 plasma etching of SiO_2, *Plasma Sources Sci. Technol*., Vol. 18 (4), 045027

(17pp), 2009.
[10] Toneli D.A., Pessoa R.S., Roberto M., Petraconi G., and Maciel H. S., *IEEE International Conference on Plasma Science (ICOPS)*, San Francisco, CA, 2013.
[11] Singh H., Coburn J.W., and Graves D. B., Measurements of neutral and ion composition, neutral temperature, and electron energy distribution function in a CF_4 inductively coupled plasma, *J. Vac. Sci. Technol. A*, Vol. 19 (3), pp. 718–729, 2001.
[12] Chun I., Efremov A., Yeom G. Y., and Kwon K.-H., A comparative study of $CF_4/O_2/Ar$ and $C_4F_8/O_2/Ar$ plasmas for dry etching applications, *Thin Solid Films*, Vol. 579, pp. 136–143, 2015.
[13] Efremov A., Lee J., and Kim J., On the control of plasma parameters and active species kinetics in $CF_4 + O_2 + Ar$ gas mixture by CF_4/O_2 and O_2/Ar mixing ratios, *Plasma Chem Plasma Process*, Vol. 37 (5), pp. 1445–1462, 2017.
[14] Conesa J.A., and Font R., Polytetrafluoroethylene decomposition in air and nitrogen, *Polymer Eng. Sci*., Vol. 41 (12), pp. 2137–2147, 2001.
[15] Fendel P., Francis A., and Czarnetzki U., Sources and sinks of CF and CF_2 in a cc-RF CF_4-plasma under various conditions, *Plasma Sources Sci. Technol*., Vol. 14 (1), pp. 1–11, 2005.
[16] Gaboriau F., Cartry G., Peignon M.-C., and Ch. Cardinaud, Etching mechanisms of Si and SiO_2 in fluorocarbon ICP plasmas: analysis of the plasma by mass spectrometry, Langmuir probe and optical emission spectroscopy, *J. Phys. D: Appl. Phys*., Vol. 39 (9), pp. 1830–1845, 2006.
[17] Tezani L. L., Pessoa R. S., Petraconi G., and Maciel H.S., Conference paper, International Plasma Chemistry Society, ISPC 20, Philadelphia, USA, 2011.
[18] Laturnus F., Haselmann K.F., Broch T., and Grøn C., Terrestrial natural sources of trichloromethane (chloroform, $CHCl_3$) – An overview, *Biogeochem.*, Vol. 60, pp. 121–139, 2002.
[19] K. Hintzer and W. Schwertfeger, Handbook of Fluoropolymer Science and Technology, First Edition, Edited by D. W. Smith Jr., S. T. Iacono, and S. S.Iyer, Hoboken, New Jersey, pp. 495 – 520, 2014.
[20] Lohmann R., Cousins I.T., DeWitt J.C., Glüge J., Goldenman G., Herzke D., Lindstrom A.B, Miller M.F., Ng C.A., Patton S., Scheringer M., Trier X., and Wang Z., Are fluoropolymers really of low concern for human and environmental health and separate from other PFAS?, *Environ. Sci. Technol*., Vol. 54 (20), pp. 12820−12828, 2020.
[21] Wang Z., DeWitt J.C., Higgins C.P., and Cousins T., A never-ending story of per- and polyfluoroalkyl substances (PFASs)?, *Environ. Sci. Technol*., Vol. 51 (5), pp. 2508−2518, 2017.
[22] Fromme H., Wöckner M., Roscher E., and Völkel W., ADONA and perfluoroalkylated substances in plasma samples of German blood donors living in South Germany*, Int. J. Hyg. Environ. Health*, Vol. 220 (2), pp. 455–460, 2017.
[23] https://www.oekobaudat.de/OEKOBAU.DAT/datasetdetail/process.xhtml?lang=de&uuid=f281ecaf-5754-4d27-8d70-cfd18780b192&version=20.19.120, retrieved on 15*th* December, 2021.